Available online at www.sciencedirect.com

ScienceDirect

Nuclear Physics B 923 (2017) 245–257

NUCLEAR PHYSICS B

www.elsevier.com/locate/nuclphysb

Minimal flavor-changing Z' models and muon $g-2$ after the R_{K^*} measurement

Stefano Di Chiara [a], Andrew Fowlie [b], Sean Fraser [a,*], Carlo Marzo [a], Luca Marzola [a], Martti Raidal [a], Christian Spethmann [a]

[a] *National Institute of Chemical Physics and Biophysics, Rävala 10, Tallinn 10143, Estonia*

[b] *ARC Centre of Excellence for Particle Physics at the Tera-scale, School of Physics and Astronomy, Monash University, Melbourne, Victoria 3800, Australia*

Received 15 May 2017; received in revised form 25 July 2017; accepted 5 August 2017
Available online 10 August 2017
Editor: Hong-Jian He

Abstract

There has been a steady interest in flavor anomalies and their global fits as ideal probes of new physics. If the anomalies are real, one promising explanation is a new Z' gauge boson with a flavor-changing coupling to bottom and strange quarks and a flavor-conserving coupling to muons and, possibly, electrons. We point out that direct production of such a Z', emerging from the collision of b and s quarks, may offer a complementary window into these phenomena because collider searches already provide competitive constraints. On top of that, we analyze the same Z' scenario in relation to another long-standing discrepancy between theory and experiment that concerns the anomalous magnetic moment of the muon. By scanning the allowed Z' coupling strengths in the low-mass region, we assess the compatibility of the signals from LHCb with the Z' searches in the high energy LHC data and the measurements of the anomalous magnetic moments of the involved leptons. We also argue that observations of the latter can break the degeneracy pattern in the Wilson coefficients C_9 and C_{10} presented by LHCb data. The Z' model we consider is compatible with the new measurement of R_{K^*}, therefore it can potentially account for the long-standing deviations observed in B-physics.

* Corresponding author.
E-mail address: sean.fraser@kbfi.ee (S. Fraser).

http://dx.doi.org/10.1016/j.nuclphysb.2017.08.003
0550-3213/

1. Introduction

Processes involving flavor-changing neutral currents are sensitive probes of new physics. In the Standard Model (SM), transitions such as $b \to s\ell^+\ell^-$ are loop-suppressed, but new particles can contribute at tree-level. The possible impact of new particles on these processes is usually analyzed by integrating out the heavy degrees of freedom and working with the effective Hamiltonian. For $b \to s$ transitions we have

$$\mathcal{H}_{\text{eff}} = -\frac{4G_F}{\sqrt{2}} \frac{e^2}{16\pi^2} V_{tb} V_{ts}^* \sum_i (C_i O_i + C_i' O_i') + H.c., \tag{1}$$

which is expressed in terms of the effective operators O_i, O_i' and the Wilson coefficients C_i, C_i'. Several anomalies with respect to SM predictions have been measured, typically at the 2σ level, but with increasing statistical significance. One notable anomaly of lepton flavor universality has occurred in the ratio of branching fractions

$$R_K = \frac{\mathcal{B}(B^+ \to K^+\mu^+\mu^-)}{\mathcal{B}(B^+ \to K^+e^+e^-)}. \tag{2}$$

The LHCb measurement [1]

$$R_K^{\text{exp}} = 0.745^{+0.090}_{-0.074} \pm 0.036 \quad \text{for } 1\ \text{GeV}^2 \leq q^2 \leq 6\ \text{GeV}^2, \tag{3}$$

where q^2 is the dilepton invariant mass squared and errors are statistical and systematic respectively, is in tension with the SM prediction[1]

$$R_K^{\text{SM}} = 1.0004 \pm 0.0002, \tag{4}$$

where the error results from propagating errors in SM parameters. Furthermore, an anomaly has appeared in a similar observable,

$$R_{K^*} = \frac{\mathcal{B}(B^0 \to K^{*0}\mu^+\mu^-)}{\mathcal{B}(B^0 \to K^{*0}e^+e^-)}, \tag{5}$$

which was recently measured by LHCb [3]

$$R_{K^*}^{\text{exp}} = \begin{cases} 0.66^{+0.11}_{-0.07} \pm 0.03 & \text{for } 0.045\ \text{GeV}^2 \leq q^2 \leq 1.1\ \text{GeV}^2 \\ 0.69^{+0.11}_{-0.07} \pm 0.05 & \text{for } 1.1\ \text{GeV}^2 \leq q^2 \leq 6\ \text{GeV}^2 \end{cases}. \tag{6}$$

There is again tension with the SM predictions

$$R_{K^*}^{\text{SM}} = \begin{cases} 0.926 \pm 0.003 \\ 0.9965 \pm 0.0005 \end{cases}. \tag{7}$$

These anomalies have already prompted several studies [4–11]. Angular observables have become a popular testing ground, and recent updates [12,13] have confirmed previous measurements in the decay $B^0 \to K^{*0}\mu^+\mu^-$. Including other transitions and a large number of observables, global fits to the anomalies seem to be converging on preferred sets of Wilson coefficients [2,14,15]. However, it is not yet entirely clear which of these sets could be responsible for the

[1] SM predictions were calculated with `flavio-0.21.2` [2].

anomalies. For example, refinement of the hadronic uncertainty in these analyses is an ongoing theoretical issue [16].

The general features of a Z' gauge boson [17] make it a good choice to generate $b \to s\ell^+\ell^-$ transitions, as underlined by many previous studies [18–32]. Most works consider Z' mass in the TeV range and above, with tree-level couplings to muons and quarks, although broad mass ranges [18,19] and radiative couplings [20] have also been considered. This includes renormalizable models based on various $U(1)$ gauge symmetries [18–22] as well as models based on extra dimensions [23–27]. From the low energy perspective, an effective theory is often useful [28–32], with minimal assumptions about the underlying details. This is the approach adopted in this work. Rather than exploring the high mass range, we focus on the sub-TeV region. One motivation for this is that contributions to the muon magnetic moment from a high mass Z' are typically too small to explain the discrepancy with the SM, although this can be overcome [20,25,32].

Most works include collider constraints similar to those that we consider. However, we provide an update by using the most recent ATLAS data, and also examine several scenarios directly related to the recent R_{K^*} measurement. Specifically, we examine the sensitivity of the Wilson coefficients to constraints from the direct production of a suitable Z' gauge boson that can also explain the discrepancy between the measured value of the muon magnetic moment and the SM prediction.

We will focus here on scenarios in which the supposed new physics contributions affect exclusively C_9^ℓ and C_{10}^ℓ, for $\ell = \mu, e$. These coefficients are among those currently favored by global fits to the anomalies [2], as well as by a recent analysis [5], which examines compatibility with R_K and the new measurement of R_{K^*}. The relevant operators are

$$O_9^\ell = (\bar{s}\gamma_\mu P_L b)(\bar{\ell}\gamma^\mu \ell) \quad \text{and} \quad O_{10}^\ell = (\bar{s}\gamma_\mu P_L b)(\bar{\ell}\gamma^\mu \gamma_5 \ell). \tag{8}$$

Another motivation for this choice is that although the measurements of R_{K^*} and R_K suggest there is new physics which discriminates between muons and electrons, the LHCb data currently exhibit an interesting degeneracy in C_9^ℓ and C_{10}^ℓ based on their statistical pulls [5]: we argue that such degeneracy can be broken by analyses of the magnetic moments of the involved leptons in scenarios where the considered Z' boson is well below the TeV scale. In addition, our analysis will show that the LEP bounds strongly disfavor scenarios where the speculated Z' boson couples purely to electrons, besides quarks.

After introducing the adopted framework and detailing our methodology in Section 2, we present the results of our analysis in Section 3. Our conclusions are offered in Section 4.

2. A simple Z' model

We assume a general interaction of a Z' boson with quarks $\bar{s}b$ and leptons $\bar{\ell}\ell$ described by the Lagrangian

$$\mathcal{L} \supset \frac{g_2}{2c_W} Z'_\alpha \left\{ \left[\bar{s}\gamma^\alpha (g_L^q P_L + g_R^q P_R) b + h.c. \right] + \bar{\ell}\gamma^\alpha (g_V^\ell + \gamma_5 g_A^\ell)\ell \right\}, \tag{9}$$

where $\ell = \mu, e$. The companion interactions with neutrinos and up-type quarks are allowed by the SM gauge symmetry and may offer interesting features which, however, we do not pursue in this work. The quark flavor-violating couplings g_L^q, g_R^q and the lepton flavor-conserving couplings g_V^ℓ, g_A^ℓ are normalized relative to $g_2/(2c_W)$ from the Standard Model for convenience, c_W being the cosine of the Weinberg angle.

The above Lagrangian should be considered as an effective low energy description of new physics. A UV-complete theory of a massive Z' gauge boson must contain an associated Higgs sector, and the existence of non-diagonal couplings to the heavy gauge boson requires mixing of the quark fields, with potential consequences for the CKM matrix. In addition, since we will consider $g_L^q \neq g_R^q$, new fermions are required for the cancellation of chiral anomalies. The new scalars and fermions would also produce additional contributions to other low energy operators, which might be relevant for the phenomenology of the theory. In this work we pursue a minimal approach, and assume that these new states are too heavy to affect our results. This can in principle always be achieved by tuning the parameters of the underlying theory. We refer the reader to Ref. [33] for a thorough discussion of these issues.

After integrating out the Z' and performing tree-level matching, the Wilson coefficients bounded by the LHCb results are related to the Z' couplings by

$$\frac{e^2}{16\pi^2} V_{tb} V_{ts}^* \cdot \left\{ C_9^\ell,\, C_{10}^\ell,\, C_9'^{\,\ell},\, C_{10}'^{\,\ell} \right\} = \frac{M_Z^2}{2M_{Z'}^2} \cdot \left\{ g_L^q g_V^\ell,\, g_L^q g_A^\ell,\, g_R^q g_V^\ell,\, g_R^q g_A^\ell \right\}. \tag{10}$$

The Wilson coefficient C_9^ℓ and $C_9'^{\,\ell}$ encapsulate the vectorial couplings between the Z' and leptons, whereas C_{10}^ℓ and $C_{10}'^{\,\ell}$ contain the axial couplings. As we can see, despite its simplicity, the Z' model at hand can potentially account for deviations from lepton flavor universality.

As mentioned earlier, according to Ref. [5] the contributions from $C_9'^{\,\ell}$ and $C_{10}'^{\,\ell}$ are less favored by experiments, compared to the unprimed Wilson coefficients, and for this reason we set the former two equal to zero by taking $g_R^q = 0$ in Eqs. (9) and (10). The Wilson coefficients are matched at the scale m_b. We checked with `flavio` that running between m_b and $M_{Z'}$ induces changes in the Wilson coefficients of less than about 5% for Wilson coefficients that explain the anomalies.[2]

The Z' contributions to the magnetic moment of a charged lepton $\ell = \mu, e$ are given by

$$\Delta_{g-2}^\ell = \frac{1}{12\pi^2} \left(\frac{g_2\, g_V^\ell}{2c_W} \right)^2 \frac{m_\ell^2}{M_{Z'}^2}\,, \tag{11}$$

for C_9 scenarios, and by

$$\Delta_{g-2}^\ell = -\frac{5}{12\pi^2} \left(\frac{g_2\, g_A^\ell}{2c_W} \right)^2 \frac{m_\ell^2}{M_{Z'}^2}\,, \tag{12}$$

for C_{10} scenarios, where $M_{Z'}$ is the mass of Z'. In our analysis we will refer to the following values for the measured discrepancies of the involved lepton magnetic moments: $\Delta_{g-2}^e = (-10.5 \pm 8.1) \times 10^{-13}$, $\Delta_{g-2}^\mu = (290 \pm 90) \times 10^{-11}$ [35,36].

With $g_R^q = 0$, the parameters to be scanned over are $M_{Z'}$ and the set of couplings

$$g_L^q,\, g_V^\ell \text{ and } g_A^\ell, \tag{13}$$

which are for instance subject to the LHC dilepton searches that provide upper bounds on the production cross section times branching ratio as a function of $M_{Z'}$, $\sigma_{\ell\ell} \equiv \sigma(pp \to Z') \cdot \mathcal{B}(Z' \to$

[2] `flavio` includes complete NNLO QCD and NLO EW running, except for C_9, for which NLO EW corrections are only partially known (see Ref. [34]).

$\ell^+\ell^-$). Using the interaction Lagrangian above with specified input values of the Z' mass and couplings, we numerically simulate the dilepton searches, yielding the constraint

$$\sigma^{\rm sim}_{\ell\ell}(M_{Z'}, g^q_L, g^\ell_V) \le \sigma^{\rm exp}_{\ell\ell}(M_{Z'}), \tag{14}$$

for C_9 scenarios, and

$$\sigma^{\rm sim}_{\ell\ell}(M_{Z'}, g^q_L, g^\ell_A) \le \sigma^{\rm exp}_{\ell\ell}(M_{Z'}), \tag{15}$$

for C_{10} scenarios, where $\sigma^{\rm sim}_{\ell\ell}$ is the result of our simulation and $\sigma^{\rm exp}_{\ell\ell}$ is the experimental upper bound. Specifically, we simulate the center of mass energy and integrated luminosity of the most recent ATLAS search [37] with the associated selection requirements. These include pseudorapidity $|\eta| < 2.5$ and transverse momentum $p_T > 30$ GeV for leptons. The angular isolation requirement is $\Delta R \ge 0.4$ and the dilepton invariant mass cut is $|M_{\ell\ell} - M_{Z'}| \le 3\Gamma_{Z'}$. The Z' width is $\Gamma_{Z'} \sim 10$ GeV for couplings $g^q_L, g^\ell_V, g^\ell_A \sim 1$ and $M_{Z'} = 500$ GeV.

In any given scenario, the quark coupling g^q_L controls $\sigma(pp \to Z')$ but also affects $\mathcal{B}(Z' \to \ell^+\ell^-)$ since the width $\Gamma_{Z'}$ includes both dilepton and dijet decay channels. As a conservative choice, we impose the full ATLAS bound by only simulating the interactions with s, b quarks and the relevant charged lepton pair. Including the remaining interactions allowed by the SM gauge invariance with c, t quarks and neutrinos would not significantly affect production but would reduce the Z' branching ratio to charged leptons, thereby weakening the constraint. These conclusions may not hold in extensions of the current framework when additional couplings to u, d quarks are included, which would for instance affect production. For a previous analysis, we refer to Ref. [32].

The most stringent limits on the couplings of the Z' to electrons originate from LEP electroweak precision measurements [38]. Integrating out the Z' in our model generates the effective four-fermion operators

$$\mathcal{L}_{\rm eff} \supset \frac{1}{2}\left(\frac{g_2}{2c_W}\right)^2 \left(\frac{g^e_V}{M_{Z'}}\right)^2 (\bar{e}\gamma_\mu e)(\bar{e}\gamma^\mu e), \tag{16}$$

and

$$\mathcal{L}_{\rm eff} \supset \frac{1}{2}\left(\frac{g_2}{2c_W}\right)^2 \left(\frac{g^e_A}{M_{Z'}}\right)^2 (\bar{e}\gamma_\mu \gamma_5 e)(\bar{e}\gamma^\mu \gamma_5 e), \tag{17}$$

which are constrained by measurements of $e^+e^- \to e^+e^-$ cross sections at LEP. The upper limits on the magnitudes of the electron–Z' couplings are

$$|g^e_V| \le \frac{2c_W}{g_2}\sqrt{4\pi}\,\frac{M_{Z'}}{20.6\ \text{TeV}} \quad \text{and} \quad |g^e_A| \le \frac{2c_W}{g_2}\sqrt{4\pi}\,\frac{M_{Z'}}{10.1\ \text{TeV}}, \tag{18}$$

which respectively hold in the case of vectorial and axial couplings.

We scan the allowed range of couplings for two different masses of Z', with the values $M_{Z'} =$ 200 GeV, 500 GeV for scenarios involving muons, and $M_{Z'} = 250$ GeV, 500 GeV for those involving electrons. Our simulations were performed using `MadGraph_aMC5@NLO` [39] and we validated our code in the special case of a sequential Z' against the simulated cross section reported in Ref. [37] as a function of $M_{Z'}$.

In our analyses we consider also the constraint from B^0_s–$\bar{B}^0_s$ oscillations in terms of the measured mass difference ΔM_s given by [40]

$$\frac{\Delta M_s}{\Delta M_s^{\rm SM}} \simeq 1 + \frac{M_Z^2}{M_{Z'}^2}\left[(g_L^q)^2 + (g_R^q)^2 - 9.7(g_L^q)(g_R^q)\right]\left(\frac{g_2^2}{16\pi^2}(V_{ts}^* V_{tb})^2 S_0\right)^{-1}, \tag{19}$$

where the contribution from the second term on the right-hand side is bounded by experiment to be in magnitude below the 10% level. The SM loop function is $S_0 \simeq 2.3$ and the above expression is based on the results for the hadronic matrix elements presented in Ref. [29].

As for the low-energy observations, including recent measurements by LHCb, we remark that a comprehensive statistical analysis of the Wilson coefficients would involve about 100 observables and a careful treatment of about 100 nuisance parameters. This is so technically challenging that instead approximate "fast-fit" techniques are favored (see e.g., [5,6]), although they require considerable computing resources. Since a comprehensive analysis is beyond the purpose of this paper, we adopt a pragmatic approach to understand the impact of the latest data. We perform an independent fit of the Wilson coefficients to LHCb measurements of R_{K^*} [3] and R_K [1], Belle measurements of D_4' and D_5' [41], and LHCb measurements of $\mathcal{B}(B_s^0 \to \mu^+\mu^-)$ and $\mathcal{B}(B^0 \to \mu^+\mu^-)$ [42]. Recent studies [6,8] performed global frequentist statistical analysis, whereas [9] performed a global Bayesian analysis with a subset of nuisance parameters and data with `HEPfit` [43]. Our methodology and its results are detailed in the next section.

3. A first analysis

We calculated the profile likelihood with `MultiNest` [44] interfaced with a modified version of `flavio` [2]. Confidence intervals were found by Wilks' theorem (see [45] for conventions and definitions). All nuisance parameters (m_b, m_c, CKM matrix elements and form factors) were fixed to their central values. Wilson coefficients were varied between -5 and 5 at the scale m_b. We find reasonable agreement for best-fits, confidence intervals and significances with similar `flavio` results with Markov Chain Monte Carlo algorithms and fast-fit techniques for nuisance parameters [5]. We estimate the significance of the preference for new physics versus the SM to be about 4.5σ, in agreement with recent literature [4–6,8,9], but, as in the literature, there are important caveats about systematic uncertainties.

Since it is a product of our `MultiNest` fit, we note that data favor the C_9^μ model by a Bayes factor of about 10^4 versus the SM and about 10 versus C_{10}^μ, as well as versus C_9^e or C_{10}^e. Since, however, we omitted important nuisance parameters that may alleviate tension in the SM, 10^4 should be regarded as an upper bound to the Bayes factor versus the SM (and is, of course, sensitive to priors). A Bayes factor preference for C_9^μ versus electron Wilson coefficients was also noted in an earlier study of R_K [46].

The results we obtained are presented in Fig. 1, whereas Table 1 proposes the results from Ref. [5] for comparison. We find that the two analyses are in reasonable agreement given that the fits take into account different sets of observables.

We focus now on the constraints that collider and low energy experiments impose on the scenarios we delineated.

3.1. Scenarios with C_9^e or C_{10}^e only

We present in Fig. 2 the results obtained for the scenario where new physics effects arise from the coupling of Z' to electrons, and the relative effects are fully encapsulated in the Wilson

Table 1
The values obtained for the Wilson coefficients from a fit to $b \to s\bar{\ell}\ell$ anomalies in Ref. [5].

Coeff.	best fit	1σ CL	2σ CL
C_9^μ	-1.59	$[-2.15, -1.13]$	$[-2.90, -0.73]$
C_{10}^μ	$+1.23$	$[+0.90, +1.60]$	$[+0.60, +2.04]$
C_9^e	$+1.58$	$[+1.17, +2.03]$	$[+0.79, +2.53]$
C_{10}^e	-1.30	$[-1.68, -0.95]$	$[-2.12, -0.64]$

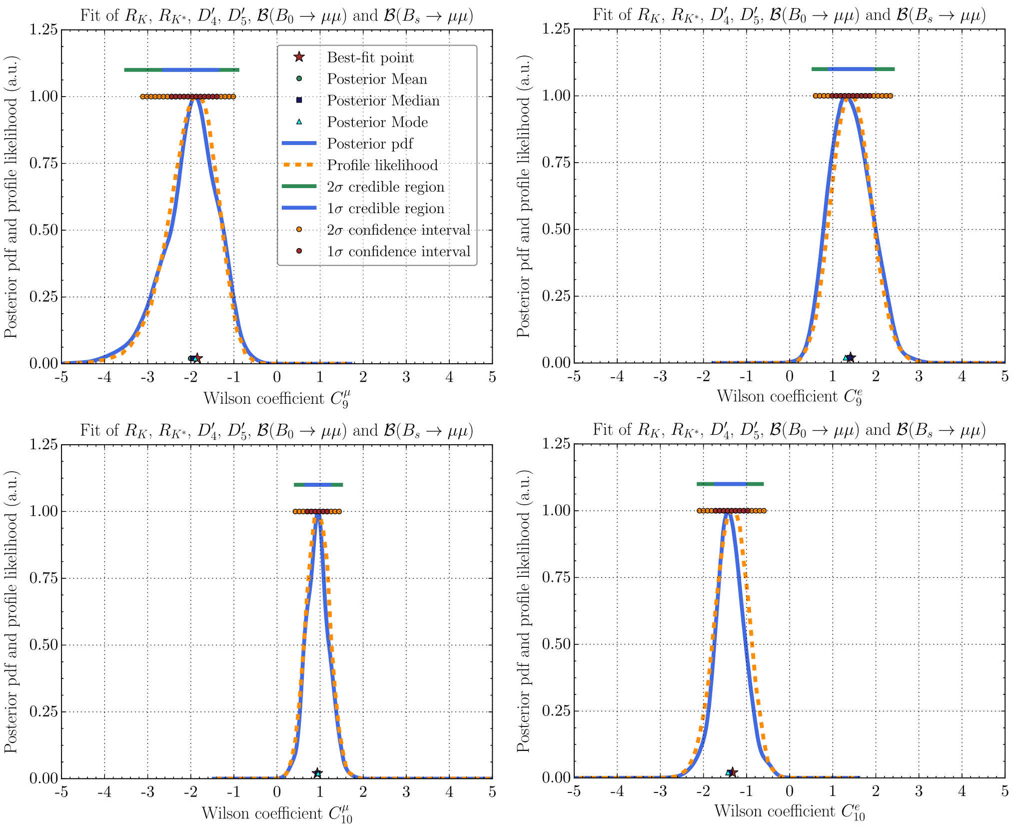

Fig. 1. Best-fits to $b \to s\ell^+\ell^-$ anomalies for the indicated Wilson coefficients at the scale m_b.

coefficient C_9^e (top panels), or C_{10}^e (bottom panels). The different shaded areas indicate allowed regions of parameter space after taking into account the various constraints.

The green area represents the region allowed by the ATLAS Z' searches in the dielectron channel. The blue band represents the values of the coupling selected by the LHCb measurements of the indicated Wilson coefficient. We refer here to the values for the 2σ credible regions from our analysis presented in Fig. 1. The red band illustrates instead the region of the parameter space allowed by the constraints on the mass difference ΔM_s.

As mentioned before, we also checked that the Z' contribution to the electron $g-2$ does not spoil the current agreement between theory and experiment. A plot of the new contribution

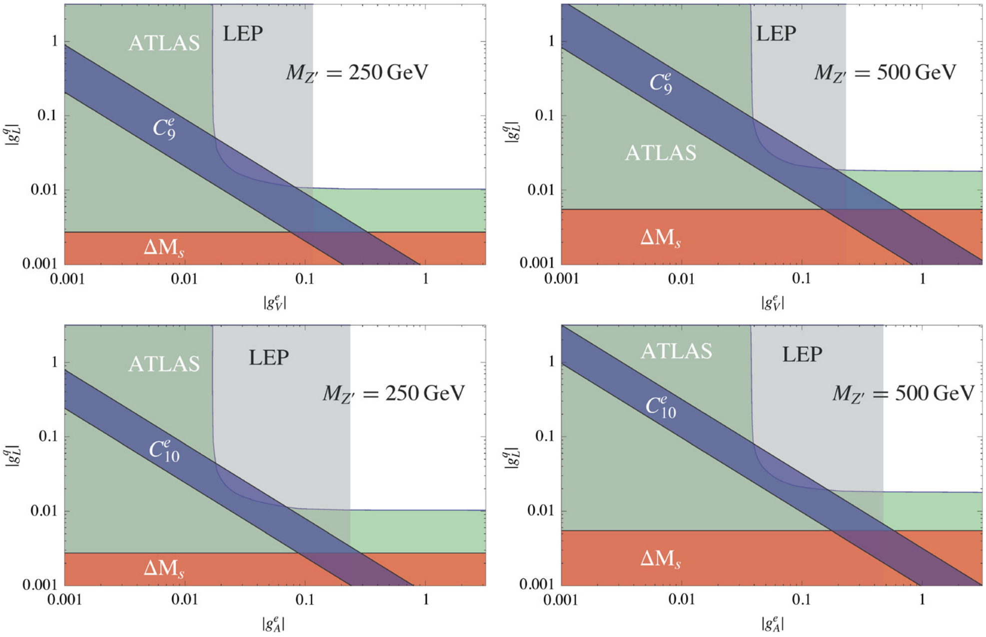

Fig. 2. Experimental constraints on the scenario where the Z' only couples to electrons, with $g_R^q = 0$. The shaded regions correspond to the allowed regions of parameter space. Upper panels: C_9^e is non-zero and generated by a Z' with mass 250 GeV (left) and 500 GeV (right). Lower panels: C_{10}^e is non-zero and generated by a Z' with mass 250 GeV (left) and 500 GeV (right). (For interpretation of the references to color in this figure, the reader is referred to the web version of this article.)

to this quantity is presented in Fig. 3 as a function of $M_{Z'}$ for different values of the relevant coupling. The results in the top panel holds for the scenario where all the new physics effects are contained in C_9^e, the bottom one for the case of C_{10}^e. We can see that values of $M_{Z'} \lesssim 50$ GeV would negatively impact on the prediction for the anomalous magnetic moment of the electron.

We remark that these scenarios where the Z' only couples to electrons, besides quarks, are strongly constrained by the bounds from LEP-II [38]. The gray shade in Fig. 2 denotes the area of the parameter space that evades the latter. We can see that the scenario with non-zero C_9^e generated from a vector coupling is more tightly constrained than C_{10}^e by LEP electroweak precision measurements and B_s^0–$\bar{B}_s^0$ oscillations. Indeed, in the case of non-zero C_{10}^e a larger region of the parameter space is still allowed by all the considered experimental limits. A Z' boson with axial vector couplings would also induce a negative contribution to the $g-2$ of the electron, and is therefore amenable to reducing the tension between the measurements and the SM prediction. Although in the simple models we are considering this contribution is not substantial, we remark that the preference for C_{10}^e based on $g-2$ is consistent with the picture emerging from the other constraints analyzed.

3.2. Scenarios with C_9^μ and C_{10}^μ only

We present in Fig. 4 the analogous results obtained for the case in which, besides quarks, the speculated Z' couples exclusively to muons.

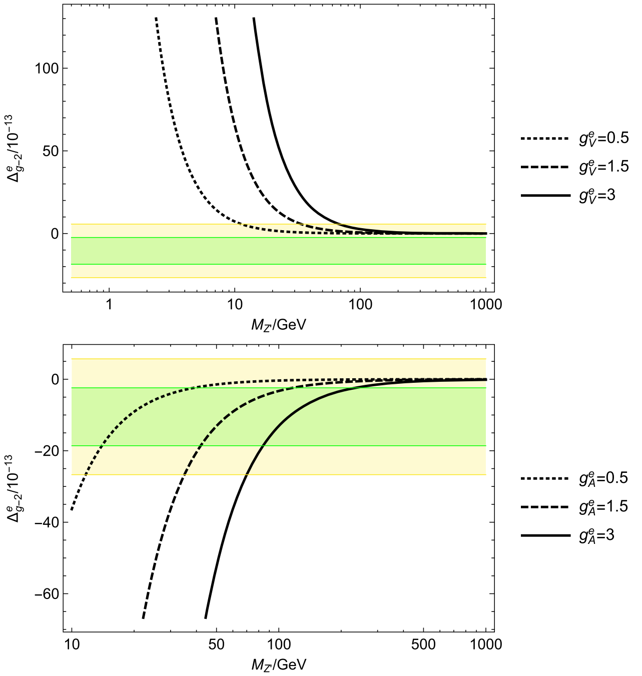

Fig. 3. The Z' contribution to the anomalous magnetic moment of the electron. The green and yellow bands represent the 1σ and 2σ confidence levels for the discrepancy between the measurement and the SM prediction. The top panel is for the scenario where all the new physics effects are contained in C_9^e, the bottom one for the case of C_{10}^e. (For interpretation of the references to color in this figure legend, the reader is referred to the web version of this article.)

Again we show in the top panel the case where new physics affects C_9^μ only, and the bottom panels cover the complementary case of C_{10}^μ. As before, the green area represents the region of the parameter space allowed by the ATLAS Z' searches, here for the dimuon channel. The blue band represents the values of the coupling selected by the LHCb measurements of the indicated Wilson coefficient, according to the 2σ credible intervals shown in Fig. 1. The red band is the region of the parameter space allowed by the constraints on the mass difference ΔM_s. We remark that LEP measurements do not constrain the couplings in these scenarios.

The Z' contribution in the C_9^μ scenario can help to bridge the discrepancy between the measured value of the muon magnetic moment and the SM prediction. As we can see in Fig. 5, the Z' contribution is potentially able to reduce such a discrepancy below the 1σ level for moderate values of the Z'-muon couplings for Z' masses up to about 250 GeV. The solid black line in this region with $g_V^\mu = 3$ and $M_{Z'} \simeq 200$ GeV is compatible with the parameter space selected by the LHCb data. In this case, the physical coupling $g_V^\mu(g_2/2c_W) \simeq 0.3\sqrt{4\pi}$ is large, but marginally within the perturbative regime. The corresponding region in Fig. 4 is allowed, when the top left panel is extrapolated to $g_L^q \simeq 10^{-4}$.

There are also upper limits on the Z' coupling to muons from neutrino trident production i.e. muon pair-production during neutrino–nucleus scattering [32]. These upper limits do not affect the overlap of the C_9^μ and ΔM_s regions shown in Fig. 4, but they would limit the Z' contribution to $g-2$. This can in principle be compensated for once a UV-completion of the

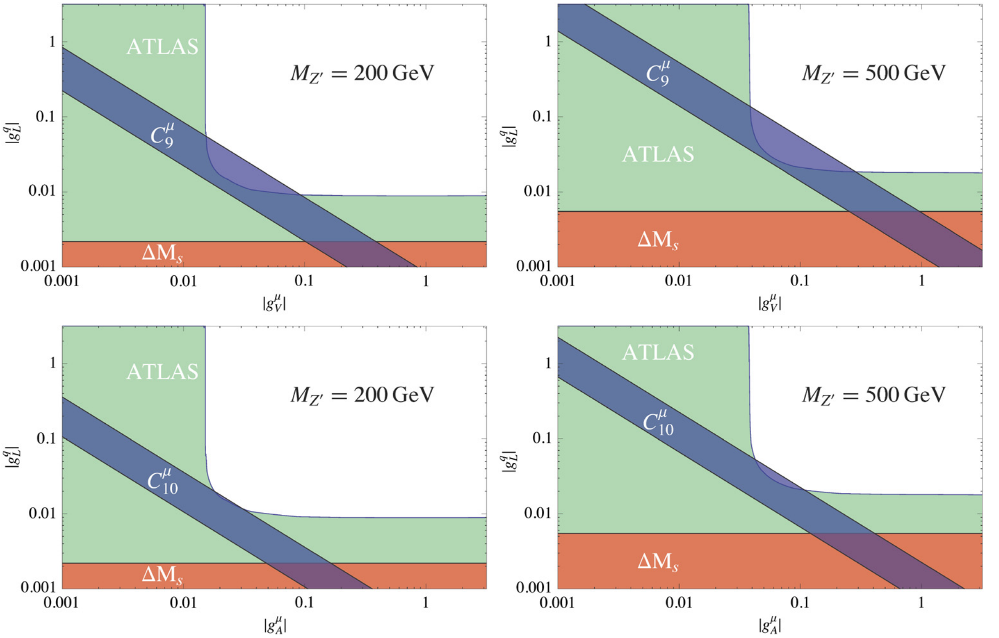

Fig. 4. Experimental constraints on the scenario where the Z' only couples to muons, with $g_R^q = 0$. The shaded regions correspond to the allowed regions of parameter space. Upper panels: C_9^μ is non-zero and generated by a Z' with mass 200 GeV (left) and 500 GeV (right). Lower panels: C_{10}^μ is non-zero and generated by a Z' with mass 200 GeV (left) and 500 GeV (right). (For interpretation of the references to color in this figure, the reader is referred to the web version of this article.)

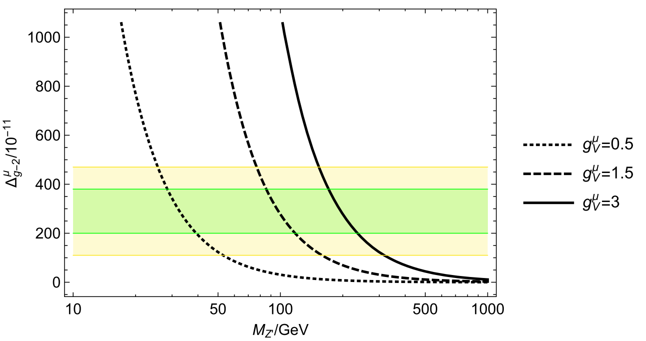

Fig. 5. The Z' contribution to the anomalous magnetic moment of the muon. The green and yellow bands represent the 1σ and 2σ confidence levels for the discrepancy between the measurement and the SM prediction. (For interpretation of the references to color in this figure legend, the reader is referred to the web version of this article.)

theory is assumed, which can provide non-negligible contributions to $g-2$ if the new states are not excessively heavy.

As for the C_{10}^μ case (not shown), the presence of a Z' in the low-mass range can only worsen the theory prediction as the relative contribution, of negative sign, further lowers the value of the latter.

4. Conclusions

In this paper we considered four different new physics scenarios which could explain the anomalous B-physics results from LHCb and argued that measurements of the anomalous magnetic moments of muon and electron could break the degeneracy in the $C_9^{\mu(e)}$–$C_{10}^{\mu(e)}$ Wilson coefficients.

We find that a Z'-boson which couples only to electrons can produce the correct values for R_K and R_{K^*}, but such a scenario is strongly constrained by the precision measurements from LEP. However, if the Z' coupling to e^+e^- is purely axial, the allowed region of parameter space is larger. Such an axially coupled Z' also generates a negative contribution to the anomalous magnetic moment of the electron and a more sophisticated version of the minimal model could therefore potentially accommodate both anomalies.

We also considered scenarios where the Z'-boson couples only to muons. In this case, a vectorial coupling to the Z' is favored by the Bayesian approach employed for the performed fit. Such a scenario produces also a positive contribution to the $g-2$ of the muon and therefore could help to alleviate the tension between the $g-2$ measurement and the SM prediction. This scenario can also explain the LHCb anomalies while avoiding all the remaining constraints from high energy searches, provided the vectorial coupling to muons is large ($g_V^\mu > 0.1$). An axial coupling of the Z' to muons can also explain the LHCb results, but increases the disagreement of the $g-2$ with measurements.

Acknowledgements

We thank Christian Veelken for useful discussions. This work was supported by the Estonian Research Council grant IUT23-6 and by the EU through the ERDF CoE program grant TK133. The work of CM is supported by the "Angelo Della Riccia" foundation.

References

[1] R. Aaij, et al., Test of lepton universality using $B^+ \to K^+\ell^+\ell^-$ decays, Phys. Rev. Lett. 113 (2014) 151601, http://dx.doi.org/10.1103/PhysRevLett.113.151601, arXiv:1406.6482.
[2] W. Altmannshofer, C. Niehoff, P. Stangl, D.M. Straub, Status of the $B \to K^*\mu^+\mu^-$ anomaly after Moriond 2017, arXiv:1703.09189.
[3] R. Aaij, et al., Test of lepton universality with $B^0 \to K^{*0}\ell^+\ell^-$ decays, arXiv:1705.05802.
[4] B. Capdevila, A. Crivellin, S. Descotes-Genon, J. Matias, J. Virto, Patterns of New Physics in $b \to s\ell^+\ell^-$ transitions in the light of recent data, arXiv:1704.05340.
[5] W. Altmannshofer, P. Stangl, D.M. Straub, Interpreting hints for lepton flavor universality violation, arXiv:1704.05435.
[6] G. D'Amico, M. Nardecchia, P. Panci, F. Sannino, A. Strumia, R. Torre, A. Urbano, Flavour anomalies after the R_{K^*} measurement, arXiv:1704.05438.
[7] G. Hiller, I. Nisandzic, R_K and R_{K^*} beyond the Standard Model, arXiv:1704.05444.
[8] L.-S. Geng, B. Grinstein, S. Jäger, J. Martin Camalich, X.-L. Ren, R.-X. Shi, Towards the discovery of new physics with lepton-universality ratios of $b \to s\ell\ell$ decays, arXiv:1704.05446.
[9] M. Ciuchini, A.M. Coutinho, M. Fedele, E. Franco, A. Paul, L. Silvestrini, M. Valli, On flavourful Easter eggs for New Physics hunger and lepton flavour universality violation, arXiv:1704.05447.
[10] D. Bečirević, O. Sumensari, A leptoquark model to accommodate $R_K^{\rm exp} < R_K^{\rm SM}$ and $R_{K^*}^{\rm exp} < R_{K^*}^{\rm SM}$, arXiv:1704.05835.
[11] A. Celis, J. Fuentes-Martin, A. Vicente, J. Virto, Gauge-invariant implications of the LHCb measurements on lepton-flavour non-universality, arXiv:1704.05672.
[12] Angular analysis of $B_d^0 \to K^*\mu^+\mu^-$ decays in pp collisions at $\sqrt{s} = 8$ TeV with the ATLAS detector, Tech. Rep. ATLAS-CONF-2017-023, CERN, Geneva, Apr 2017, URL http://cds.cern.ch/record/2258146.

[13] Measurement of the P_1 and P'_5 angular parameters of the decay $B^0 \to K^{*0}\mu^+\mu^-$ in proton–proton collisions at $\sqrt{s} = 8$ TeV, Tech. Rep. CMS-PAS-BPH-15-008, CERN, Geneva, 2017, URL http://cds.cern.ch/record/2256738.

[14] S. Descotes-Genon, J. Matias, J. Virto, Understanding the $B \to K^*\mu^+\mu^-$ anomaly, Phys. Rev. D 88 (2013) 074002, http://dx.doi.org/10.1103/PhysRevD.88.074002, arXiv:1307.5683.

[15] S. Descotes-Genon, L. Hofer, J. Matias, J. Virto, Global analysis of $b \to s\ell\ell$ anomalies, J. High Energy Phys. 06 (2016) 092, http://dx.doi.org/10.1007/JHEP06(2016)092, arXiv:1510.04239.

[16] S. Descotes-Genon, L. Hofer, J. Matias, J. Virto, On the impact of power corrections in the prediction of $B \to K^*\mu^+\mu^-$ observables, J. High Energy Phys. 12 (2014) 125, http://dx.doi.org/10.1007/JHEP12(2014)125, arXiv:1407.8526.

[17] P. Langacker, The physics of heavy Z' gauge bosons, Rev. Mod. Phys. 81 (2009) 1199–1228, http://dx.doi.org/10.1103/RevModPhys.81.1199, arXiv:0801.1345.

[18] A. Crivellin, G. D'Ambrosio, J. Heeck, Explaining $h \to \mu^\pm\tau^\mp$, $B \to K^*\mu^+\mu^-$ and $B \to K\mu^+\mu^-/B \to Ke^+e^-$ in a two-Higgs-doublet model with gauged $L_\mu - L_\tau$, Phys. Rev. Lett. 114 (2015) 151801, http://dx.doi.org/10.1103/PhysRevLett.114.151801, arXiv:1501.00993.

[19] A. Crivellin, G. D'Ambrosio, J. Heeck, Addressing the LHC flavor anomalies with horizontal gauge symmetries, Phys. Rev. D 91 (7) (2015) 075006, http://dx.doi.org/10.1103/PhysRevD.91.075006, arXiv:1503.03477.

[20] G. Bélanger, C. Delaunay, S. Westhoff, A dark matter relic from muon anomalies, Phys. Rev. D 92 (2015) 055021, http://dx.doi.org/10.1103/PhysRevD.92.055021, arXiv:1507.06660.

[21] R. Gauld, F. Goertz, U. Haisch, An explicit Z'-boson explanation of the $B \to K^*\mu^+\mu^-$ anomaly, J. High Energy Phys. 01 (2014) 069, http://dx.doi.org/10.1007/JHEP01(2014)069, arXiv:1310.1082.

[22] A.J. Buras, F. De Fazio, J. Girrbach, 331 models facing new $b \to s\mu^+\mu^-$ data, J. High Energy Phys. 02 (2014) 112, http://dx.doi.org/10.1007/JHEP02(2014)112, arXiv:1311.6729.

[23] E. Megias, M. Quiros, L. Salas, Lepton-flavor universality violation in $R_{D^{(*)}}$ and R_K from warped space, arXiv:1703.06019.

[24] E. Megias, G. Panico, O. Pujolas, M. Quiros, A natural origin for the LHCb anomalies, J. High Energy Phys. 09 (2016) 118, http://dx.doi.org/10.1007/JHEP09(2016)118, arXiv:1608.02362.

[25] E. Megias, M. Quiros, L. Salas, $g_\mu - 2$ from vector-like leptons in warped space, arXiv:1701.05072.

[26] I. Garcia Garcia, LHCb anomalies from a natural perspective, J. High Energy Phys. 03 (2017) 040, http://dx.doi.org/10.1007/JHEP03(2017)040, arXiv:1611.03507.

[27] A. Carmona, F. Goertz, Lepton flavor and nonuniversality from minimal composite Higgs setups, Phys. Rev. Lett. 116 (25) (2016) 251801, http://dx.doi.org/10.1103/PhysRevLett.116.251801, arXiv:1510.07658.

[28] A. Crivellin, L. Hofer, J. Matias, U. Nierste, S. Pokorski, J. Rosiek, Lepton-flavour violating B decays in generic Z' models, Phys. Rev. D 92 (5) (2015) 054013, http://dx.doi.org/10.1103/PhysRevD.92.054013, arXiv:1504.07928.

[29] A.J. Buras, F. De Fazio, J. Girrbach, The anatomy of Z' and Z with flavour changing neutral currents in the flavour precision era, J. High Energy Phys. 02 (2013) 116, http://dx.doi.org/10.1007/JHEP02(2013)116, arXiv:1211.1896.

[30] R. Gauld, F. Goertz, U. Haisch, On minimal Z' explanations of the $B \to K^*\mu^+\mu^-$ anomaly, Phys. Rev. D 89 (2014) 015005, http://dx.doi.org/10.1103/PhysRevD.89.015005, arXiv:1308.1959.

[31] A.J. Buras, J. Girrbach, Left-handed Z' and Z FCNC quark couplings facing new $b \to s\mu^+\mu^-$ data, J. High Energy Phys. 12 (2013) 009, http://dx.doi.org/10.1007/JHEP12(2013)009, arXiv:1309.2466.

[32] B. Allanach, F.S. Queiroz, A. Strumia, S. Sun, Z' models for the LHCb and $g - 2$ muon anomalies, Phys. Rev. D 93 (5) (2016) 055045, http://dx.doi.org/10.1103/PhysRevD.93.055045, arXiv:1511.07447.

[33] P. Ko, Y. Omura, Y. Shigekami, C. Yu, The LHCb anomaly and B physics in flavored Z' models with flavored Higgs doublets, arXiv:1702.08666.

[34] T. Blake, G. Lanfranchi, D.M. Straub, Rare B decays as tests of the Standard Model, Prog. Part. Nucl. Phys. 92 (2017) 50–91, http://dx.doi.org/10.1016/j.ppnp.2016.10.001, arXiv:1606.00916.

[35] G.F. Giudice, P. Paradisi, M. Passera, Testing new physics with the electron $g - 2$, J. High Energy Phys. 11 (2012) 113, http://dx.doi.org/10.1007/JHEP11(2012)113, arXiv:1208.6583.

[36] F. Jegerlehner, A. Nyffeler, The muon $g - 2$, Phys. Rep. 477 (2009) 1–110, http://dx.doi.org/10.1016/j.physrep.2009.04.003, arXiv:0902.3360.

[37] Search for new high-mass phenomena in the dilepton final state using 36.1 fb^{-1} of proton–proton collision data at $\sqrt{s} = 13$ TeV with the ATLAS detector, Tech. Rep. ATLAS-CONF-2017-027, CERN, Geneva, Apr 2017, URL http://cds.cern.ch/record/2259039.

[38] S. Schael, et al., Electroweak measurements in electron–positron collisions at W-boson-pair energies at LEP, Phys. Rep. 532 (2013) 119–244, http://dx.doi.org/10.1016/j.physrep.2013.07.004, arXiv:1302.3415.

[39] J. Alwall, R. Frederix, S. Frixione, V. Hirschi, F. Maltoni, O. Mattelaer, H.-S. Shao, T. Stelzer, P. Torrielli, M. Zaro, The automated computation of tree-level and next-to-leading order differential cross sections, and their matching

to parton shower simulations, J. High Energy Phys. 07 (2014) 079, http://dx.doi.org/10.1007/JHEP07(2014)079, arXiv:1405.0301.
[40] W. Altmannshofer, D.M. Straub, New Physics in $B \to K^* \mu\mu$?, Eur. Phys. J. C 73 (2013) 2646, http://dx.doi.org/10.1140/epjc/s10052-013-2646-9, arXiv:1308.1501.
[41] S. Wehle, et al., Lepton-flavor-dependent angular analysis of $B \to K^* \ell^+ \ell^-$, Phys. Rev. Lett. 118 (11) (2017) 111801, http://dx.doi.org/10.1103/PhysRevLett.118.111801, arXiv:1612.05014.
[42] R. Aaij, et al., Measurement of the $B_s^0 \to \mu^+\mu^-$ branching fraction and effective lifetime and search for $B^0 \to \mu^+\mu^-$ decays, arXiv:1703.05747.
[43] J. de Blas, et al., `HEPfit`: a code for the combination of indirect and direct constraints on high energy physics models.
[44] F. Feroz, M.P. Hobson, M. Bridges, MultiNest: an efficient and robust Bayesian inference tool for cosmology and particle physics, Mon. Not. R. Astron. Soc. 398 (2009) 1601–1614, http://dx.doi.org/10.1111/j.1365-2966.2009.14548.x, arXiv:0809.3437.
[45] A. Fowlie, M.H. Bardsley, Superplot: a graphical interface for plotting and analysing MultiNest output, Eur. Phys. J. Plus 131 (11) (2016) 391, http://dx.doi.org/10.1140/epjp/i2016-16391-0, arXiv:1603.00555.
[46] D. Ghosh, M. Nardecchia, S.A. Renner, Hint of lepton flavour non-universality in B meson decays, J. High Energy Phys. 12 (2014) 131, http://dx.doi.org/10.1007/JHEP12(2014)131, arXiv:1408.4097.